Hybrid Long-Distance Entanglement Distribution Protocol

J. B. Brask,[1] I. Rigas,[2] E. S. Polzik,[1] U. L. Andersen,[3] and A. S. Sørensen[1]

[1]QUANTOP, The Niels Bohr Institute, University of Copenhagen, 2100 Copenhagen Ø, Denmark
[2]Department of Optics, Facultad de Física, Universidad Complutense Madrid, 28040 Madrid, Spain
[3]Department of Physics, Technical University of Denmark, Building 309, 2800 Lyngby, Denmark

We propose a hybrid (continuous-discrete variable) quantum repeater protocol for long-distance entanglement distribution. Starting from states created by single-photon detection, we show how entangled coherent state superpositions can be generated by means of homodyne detection. We show that near-deterministic entanglement swapping with such states is possible using only linear optics and homodyne detectors, and we evaluate the performance of our protocol combining these elements.

Two regimes for optical quantum computation and communication are commonly identified [1,2]. In the discrete variable regime, single photons are the carriers of information with information encoded, e.g., in their polarization or frequency, and measurements are performed by single-photon detection (SPD). In the continuous variable regime, information is encoded in continuous degrees of freedom of the light field such as the field quadratures, which are measured via homodyne detection. Both regimes have their advantages and drawbacks. On the one hand, single photons are good for heralding events across lossy channels since their discrete nature implies that no partial loss can take place. Successful detection of a photon at the channel output unambiguously identifies a successful event. This is useful for entanglement generation [3,4]. On the other hand, certain tasks, such as quantum teleportation [5], can be accomplished unconditionally with linear optics in the continuous regime while not in the discrete one, and homodyne detection allows quadrature measurements with much higher efficiency than what can be achieved with SPD at present.

Quantum repeaters achieve scalable entanglement distribution across long lossy channels by first generating entanglement over shorter segments which are then connected by entanglement swapping and purification [6]. Reaching high rates thus requires both a good generation scheme and efficient swapping. Repeaters combining continuous and discrete variables have recently been proposed. Reference [7] relies on nonlinear interactions of light with single spins in cavities, which is not easy to realize experimentally. Reference [8] is based on linear optics, but makes use of inefficient single-photon counters to perform entanglement swapping. Here we describe a quantum repeater (Fig. 1) which combines entanglement generation based on SPD with continuous variable techniques to efficiently distribute states resembling

$$|\gamma'_\theta(\alpha)\rangle = e^{i\theta}|\alpha\rangle|\alpha\rangle + e^{-i\theta}|-\alpha\rangle|-\alpha\rangle, \qquad (1)$$

where $|\alpha\rangle$ is a coherent state and θ is a phase (throughout this Letter α is real). In quantum optics, coherent state superpositions of this form, and similarly for a single mode

$$|\xi'(\alpha)\rangle = |\alpha\rangle + |-\alpha\rangle, \qquad (2)$$

are often called "cat" states. Such states are useful for a number of applications in quantum information, including fault-tolerant linear optical computation and quantum teleportation [9,10]. Generating exact cat states is difficult, since it requires, e.g., very strong Kerr nonlinearities [11]. Approximate cat states can be generated by photon subtraction [12–15], but unfortunately the average photon number is usually restricted to $\lesssim 1$.

We demonstrate that near-deterministic entanglement swapping of cat states using only linear optics and homodyning is possible, and we devise an efficient probabilistic scheme for generating states with many photons and very good overlap with exact squeezed single- and two-mode cat states. Our generation scheme is reminiscent of that of Ref. [16], where creation of squeezed single-mode cat states from Fock states was demonstrated, but requires no input states with more than a single photon in each mode and takes advantage of quantum memories to significantly increase the rate. Interestingly the scheme, which produces highly non-Gaussian states, is also very similar to the Gaussification protocol of Ref. [17] but run in a nonconvergent regime. The elements of our repeater are outlined in Fig. 1. In step I, Fock state entanglement between two separated nodes is generated by means of SPD. In step II, homodyning and beam splitters are used to create two-mode cat states from the states generated in I, and in step III, the entangled cat states are swapped to larger distances. We discuss these steps one by one and then finally consider the protocol in its entirety.

As shown in Fig. 1, the entanglement generation step I can be implemented using two sources of two-mode squeezed states, realized using, e.g., parametric down-conversion crystals or ensembles of Λ-type atoms [4,18]. One photonic mode from each source impinges on a central beam splitter, and a single photon is collected as indicated.
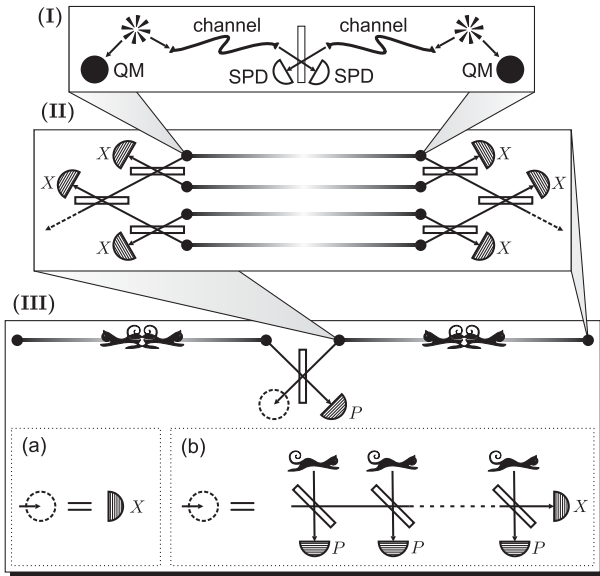
FIG. 1. (I) Generation of Bell-type entanglement between two nodes. Light from two-mode squeezing sources is mixed on a balanced beam splitter and a single photon is detected. The remaining modes are stored in quantum memories (QM). (II) Generation of approximate two-mode cat states. Pairs of Bell-like states are joined at balanced beam splitters, and the X quadrature is measured at one output of each beam splitter. When the sum of the outcomes is close to zero, the state is kept, and the process is iterated. (III) (a) Simple entanglement swapping. Two two-mode cat states are joined on a balanced beam splitter, and the outputs are homodyned. Success is conditioned on an X outcome close to zero. (b) Improved entanglement swapping using k auxiliary single-mode cat states of size (left to right) $2^{1/2}\alpha, 2\alpha, \ldots, 2^{k/2}\alpha$.

Following a single SPD click, the remaining two modes are projected to a Bell-like state [4]

$$\frac{1}{\sqrt{2}}(|01\rangle + |10\rangle) + O(\sqrt{p}), \qquad (3)$$

where the last term represents contributions from multiple excitations and is small for small pair production probability p, i.e., for weak squeezing. Because of the discrete nature of single photons, clicks herald successful transmission even for lossy channels and detectors.

In step II, states of the form (3) are combined on balanced beam splitters, and the X quadratures of two of the output modes are measured. The resulting state is kept, if the outcomes sum to a value within an interval $[-\Delta, \Delta]$. Otherwise it is discarded, and the process is restarted. Upon success, the protocol is iterated with the output states as new input states. To see that this scheme can produce catlike states, let us first consider the limit $\Delta \to 0$, $p \to 0$ and generation of a single-mode state (illustrated by, say, the left-hand side of Fig. 1 II only). We start from two sources, each producing a single excitation $|1\rangle$ corresponding to the wave function

$$\psi_0(x) = \sqrt{2}\pi^{-1/4}e^{-x^2/2}x. \qquad (4)$$

The joint wave function for both sources has the form $\psi_0(x)\psi_0(y)$. A balanced beam splitter is then applied to the pair of modes x, y, transforming the state to $\psi_0[(x+y)/\sqrt{2}]\psi_0[(x-y)/\sqrt{2}] \propto e^{-(x^2+y^2)/2}(x^2 - y^2)$, followed by a measurement of y. If we require $y = 0$, corresponding to $\Delta \to 0$, the resulting unnormalized output state takes the form $e^{-x^2/2}x^2$. The process is now iterated, combining this state with the output from another pair of sources, etc. After m iterations (in Fig. 1 II, $m = 2$), the final output state wave function becomes

$$\psi_m(x) = \Gamma(2^m + 1/2)^{-1/2}e^{-x^2/2}x^{2^m}. \qquad (5)$$

This function closely resembles the wave function of the state in Eq. (2). In fact, defining $|\xi(\alpha)\rangle$ to be the normalized single-mode cat state, we find that $|\psi_m\rangle$ is well approximated by $\hat{S}(2)|\xi(\mu_m)\rangle$, where $\mu_m = \sqrt{2^m + 1/2}$ and $\hat{S}(s)$ denotes squeezing in the variance of X by a factor of s. The output state is thus very nearly a squeezed cat state. The fidelity $|\langle\psi_m|\hat{S}(2)\xi(\mu_m)\rangle|^2$ of the actual output with respect to the squeezed cat exceeds 99% for $m \geq 2$. Squeezing does not render our states less useful. They are amplitude squeezed, making them more robust against decoherence [19], and if desired they can be unsqueezed by local operations. The required squeezing of 3 dB or less is easily accessible in experiment. If the squeezing is applied to the input Fock states, the single-mode setup corresponds to amplification of small cat states via homodyne detection [20,21]. The scheme can be generalized from a single to an arbitrary number of modes by taking the mode of the single excitations from the sources to be a superposition of some other set of modes. For example, Eq. (3) corresponds to an excitation in a symmetric superposition of two spatial modes. More generally the new mode variables form a vector $\mathbf{x}$, and the source mode is given by $\mathbf{a}^\dagger\mathbf{x}$ where $\mathbf{a}$ is a unit vector. For a pair of sources, the single-mode scheme is applied to each pair of corresponding modes and we require $|\mathbf{a}^\dagger\mathbf{y}| \leq \Delta$, where $\mathbf{y}$ is the vector of measurement outcomes. Separating out the mode determined by $\mathbf{a}$, the final state becomes $|\psi_m\rangle_\mathbf{a}|\text{vac}\rangle$, where $|\text{vac}\rangle$ is the vacuum state of the remaining modes.

Step II may be implemented entirely on traveling light beams, in which case simultaneous success for all measurements is required. The rate can, however, be significantly increased if quantum memories are employed at each level of the protocol, since then no simultaneity is required. The homodyne measurements can be performed on retrieved light fields or via quantum nondemolition measurements directly on the memories [22]. To get a nonzero probability for successful generation one needs to take a nonzero value of Δ, and there will be a trade-off between the generation rate and the output state fidelity. To illustrate the trade-off with memories, we show in Fig. 2 a numerical simulation of single-mode-cat generation,
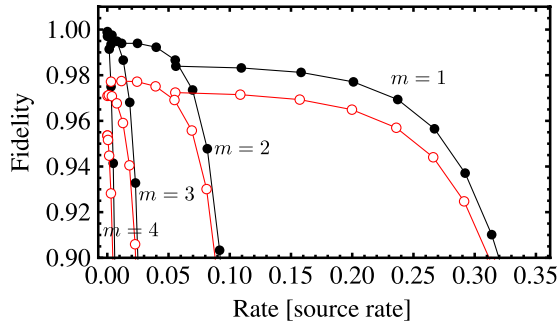
FIG. 2 (color online).   Generation of approximate cat states.
The fidelity-rate trade-off is plotted for perfect input states (dots)
and input with a 1% two-photon contribution (circles).

obtained by varying Δ, averaging over all X outcomes in
$[-\Delta, \Delta]$. Including a double excitation contribution of
1%, states with a fidelity of 90% with respect to
$\hat{S}(2)|\xi(\mu_3)\rangle$, corresponding to an unsqueezed cat ampli-
tude $\alpha = 2.9$, can be generated at a rate of ~ 0.02 times the
source rate, i.e., the rate at which (4) is produced.
Production of stored single photons is assumed much
slower than individual memory and detector operations.

As illustrated in Fig. 1 III(a), once entanglement has
been established within two neighboring segments, they
can be connected by locally mixing the modes at the
central node on a balanced beam splitter and measuring
the X and P quadratures at the two output ports. We will
first consider entanglement swapping with ideal cat states
and subsequently with the actual states produced in step II
of our scheme. We write $|\gamma_\theta(\alpha)\rangle$ for the normalized
equivalent of $|\gamma'_\theta(\alpha)\rangle$ in Eq. (1). The amount of entangle-
ment in $|\gamma_\theta(\alpha)\rangle$ varies with θ, but for coherent state
amplitudes $|\alpha|^2 \geq 2$ the variation can be safely neglected
and $|\gamma_\theta(\alpha)\rangle$ contains one ebit of entanglement. We con-
sider entanglement swapping of two copies of $|\gamma_0(\alpha)\rangle$. The
idea of the swapping procedure is that several terms in the
input state may lead to the same measurement outcome.
Conditioning on this outcome thus projects the output
modes onto an entangled superposition state. Since each
input to the beam splitter is a coherent state $|\pm \alpha\rangle$, the
possible outputs are $|\pm \sqrt{2}\alpha\rangle$ and $|0\rangle$. There are two ways
to obtain the latter, and hence measuring X and condition-
ing on an outcome close to zero results in an entangled
output state. More formally, the state prior to swapping is
$|\gamma_0(\alpha)\rangle|\gamma_0(\alpha)\rangle$. Introducing the shorthand $|\alpha_+^+\rangle = |\alpha\rangle|\alpha\rangle$,
$|\alpha_-^+\rangle = |\alpha\rangle| - \alpha\rangle$ etc., the (unnormalized) state after a
P measurement with an outcome p_0 is

$$|\alpha_-^+\rangle|\sqrt{2}\alpha\rangle_x + |\alpha_+^-\rangle| - \sqrt{2}\alpha\rangle_x + |\gamma'_{\theta_0}(\alpha)\rangle|0\rangle_x, \quad (6)$$

where we have labeled the mode for which X is measured
by x, and $\theta_0 = -2\alpha p_0$. If α is large enough for $|0\rangle$ and
$|\sqrt{2}\alpha\rangle$ to be nearly orthogonal, an X measurement with an
outcome close to zero projects the remaining modes to a
perfect two-mode cat state. Since $\langle\gamma'_{\theta_0}(\alpha)|\gamma'_{\theta_0}(\alpha)\rangle \approx 2$, the
probability for this successful outcome is roughly 1/2.

Probabilistic entanglement swapping of two-mode cat
states is thus easy to implement. As we now demonstrate,
the swapping can be made nearly deterministic using aux-
iliary single-mode cat states as a resource. The setup is
shown in Fig. 1 III(b). Additional beam splitters are
inserted between the first beam splitter output and the X
measurement. At the jth beam splitter a cat state $|\xi(2^{j/2}\alpha)\rangle$
is injected, and a P measurement with outcome p_j is
performed in one output port. We can see what happens
by considering just one auxiliary state. When the output
from the first beam splitter is mixed with a single-mode cat
of amplitude $\sqrt{2}\alpha$, each of the "failure" outputs above can
combine with one term of the cat state to yield $|0\rangle$. An
X outcome of zero then projects the output to an entangled
state. At the same time, the "success" output above splits
into $|\pm \alpha\rangle$, leading to two possible measurement out-
comes, each of which still produces the state $|\gamma'_{\theta_0}(\alpha)\rangle$.
Formally, after the two P measurements the (unnormal-
ized) state is

$$|\tilde{\gamma}'_{\theta_1}(\alpha)\rangle|0\rangle_x + |\gamma'_{\theta_0}(\alpha)\rangle(e^{i\nu}|\alpha\rangle_x + e^{-i\nu}| - \alpha\rangle_x)$$
$$+ |\alpha_-^+\rangle|2\alpha\rangle_x + |\alpha_+^-\rangle| - 2\alpha\rangle_x, \quad (7)$$

where $\theta_1 = -2^{3/2}\alpha p_1$, ν is an unimportant phase and
$|\tilde{\gamma}'_{\theta_1}(\alpha)\rangle = e^{i\theta_1}|\alpha_-^+\rangle + e^{-i\theta_1}|\alpha_+^-\rangle$ equals $|\gamma'_{\theta_1}(\alpha)\rangle$ up to a
local phase shift. Assuming that $|0\rangle$ and $|\alpha\rangle$ are nearly
orthogonal, X outcomes originating in the $|0\rangle$ or $|\pm \alpha\rangle$
terms of (7) all project the output to a two-mode cat state.
Only the extremal outcomes lead to failed swapping.
Counting terms, the success probability is 3/4.
Generalizing this to k auxiliary states, we find that the
success probability scales as $1 - 2^{-k-1}$. Fixed distinguish-
ability of the terms requires α to scale as $\alpha \sim 2^{k/2}$. The
failure probability thus scales inversely with the mean
photon number α^2 in the two-mode cats and the square
root of the mean photon number in the largest single-mode
cat. This result demonstrates that, given sufficiently large
cat-state resources, entanglement swapping using only
linear optics and homodyne measurements can be per-
formed with success probability arbitrarily close to 1.

We now turn to the assembly of all three steps—
entanglement generation I, II, and swapping III—into a
complete quantum repeater protocol. The goal is to estab-
lish a useful entangled state across some channel of length
L. To this end, the channel is divided into 2^n segments of a
shorter length L_0. Entanglement is generated in each seg-
ment separately and they are then connected by entangle-
ment swapping. We will consider only simple swapping
[Fig. 1 III(a)] with no auxiliary states, assuming that the
time required for local operations is much shorter than the
classical communication time L_0/c, with c the speed of
light. The benchmark for the performance is the rate at
which final, entangled states can be generated over a dis-
tance L with a fixed fidelity with respect to some ideal tar-
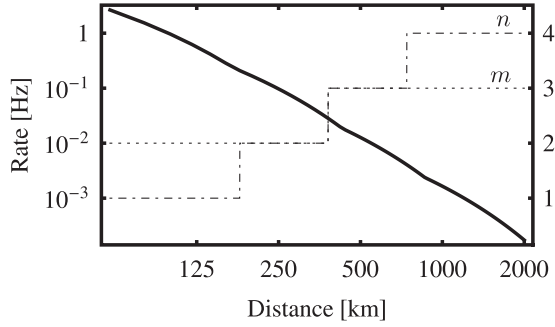get state. As in step II, one must choose a finite acceptance

FIG. 3.   Rate (solid line) of the full repeater. We assume a final fidelity of 90%, a fiber attenuation length of 20 km, and an SPD efficiency of 50%. The right-hand axis shows the optimal values of n and m.

range $[-\delta, \delta]$ for the X measurements during swapping, and for fixed L there will be a trade-off between rate and fidelity through Δ, δ, and p. The target state is approached as Δ, δ, $p \to 0$. In this limit, the entangled states before swapping are given by $|\psi_m\rangle_+|{\rm vac}\rangle_-$, where $\pm$ stand for the symmetric and antisymmetric combinations of spatial modes a, b. Conditioning on zero in all X measurements, we find that for sufficiently large m, up to two P-space displacements which can be trivially canceled, the wave function after n connections takes the form $\hat{S}_+(\frac{4}{k_n})\hat{S}_-(\frac{k_n}{2})|\gamma_{\varphi_n}(\mu_m/\sqrt{2k_n})\rangle$. Here $k_n = 2\sqrt{2}\coth[2^n{\rm arccoth}(1/\sqrt{2})]$, while φ_n depends on the P outcomes. Because k_n converges fast towards $2\sqrt{2}$, this state is essentially equivalent to $\hat{S}_a(\sqrt{2})\hat{S}_b(\sqrt{2})|\gamma_{\varphi_n}(\mu_m/2^{5/4})\rangle$. Our target is thus a squeezed, nonlocal cat state. Note that the 1.5 dB squeezing in the final state is local and can be locally undone.

We simulate the protocol stochastically, picking random outcomes for all quadrature measurements. The rate as a function of distance is maximized for a fixed final fidelity of 90% with respect to $\hat{S}_a(\sqrt{2})\hat{S}_b(\sqrt{2})|\gamma_{-\varphi_n}(\mu_m/2^{5/4})\rangle$. We optimize over the ranges Δ and δ, the number of generation and connection steps m, n, and the pair production probability p. For runtime reasons we keep $m \leq 3$. We take into account losses during entanglement generation, assuming a fiber attenuation length of 20 km and an SPD efficiency of 50%, and we take the source repetition time to be given by the classical communication time L_0/c. The result is shown in Fig. 3. At 1000 km our protocol reaches a rate of 0.1 pairs/minute. This is higher than the best proposed atomic-ensemble-based repeaters in the discrete variable regime for the same SPD efficiency. To reach comparable rates, the discrete variable protocols require high efficiency SPDs ($\gtrsim 90\%$), which unlike the efficient homodyne detectors employed here are not readily available in the lab, or more complicated entanglement swapping [23,24]. In addition, for repeaters based on linear optics and SPD in the discrete variable regime, the success probability for entanglement swapping can never exceed

1/2, whereas for the protocol presented here we have demonstrated that near-deterministic swapping and hence a much higher rate is possible when the swapping procedure of Fig. 1 III(a) is replaced by that of III(b). An analogous setup can also be used for near-deterministic teleportation. Thus the hybrid approach represents a promising avenue for reaching higher rates for entanglement distribution. Since our protocol uses only linear optics, light storage and retrieval, and single-photon and homodyne detectors, the means for a first experimental implementation are available in today's laboratories. An interesting outlook might be to integrate the present scheme with the two-mode cat generation of Ref. [8].

[1]   P. Kok *et al.*, Rev. Mod. Phys. **79**, 135 (2007).
[2]   S. L. Braunstein and P. van Loock, Rev. Mod. Phys. **77**, 513 (2005).
[3]   C. Cabrillo, J. I. Cirac, P. García-Fernández, and P. Zoller, Phys. Rev. A **59**, 1025 (1999).
[4]   L.-M. Duan, M. D. Lukin, J. I. Cirac, and P. Zoller, Nature (London) **414**, 413 (2001).
[5]   S. L. Braunstein and H. J. Kimble, Phys. Rev. Lett. **80**, 869 (1998).
[6]   H.-J. Briegel, W. Dür, J. I. Cirac, and P. Zoller, Phys. Rev. Lett. **81**, 5932 (1998).
[7]   P. van Loock *et al.*, Phys. Rev. Lett. **96**, 240501 (2006).
[8]   N. Sangouard *et al.*, J. Opt. Soc. Am. B **27**, A137 (2010).
[9]   A. P. Lund, T. C. Ralph, and H. L. Haselgrove, Phys. Rev. Lett. **100**, 030503 (2008).
[10] H. N. Phien and N. B. An, Phys. Lett. A **372**, 2825 (2008).
[11] S. Glancy and H. M. de Vasconcelos, J. Opt. Soc. Am. B **25**, 712 (2008).
[12] A. Ourjoumtsev, R. Tualle-Brouri, J. Laurat, and P. Grangier, Science **312**, 83 (2006).
[13] J. S. Neergaard-Nielsen *et al.*, Phys. Rev. Lett. **97**, 083604 (2006).
[14] H. Takahashi *et al.*, Phys. Rev. Lett. **101**, 233605 (2008).
[15] T. Gerrits *et al.*, Phys. Rev. A **82**, 031802 (2010).
[16] A. Ourjoumtsev, H. Jeong, R. Tualle-Brouri, and P. Grangier, Nature (London) **448**, 784 (2007).
[17] J. Eisert *et al.*, Opt. Spectrosc. **103**, 173 (2007).
[18] C. Simon *et al.*, Phys. Rev. Lett. **98**, 190503 (2007).
[19] A. Serafini, S. D. Siena, F. Illuminati, and M. G. A. Paris, J. Opt. B **6**, S591 (2004).
[20] A. P. Lund, H. Jeong, T. C. Ralph, and M. S. Kim, Phys. Rev. A **70**, 020101(R) (2004).
[21] M. Takeoka and M. Sasaki, Phys. Rev. A **75**, 064302 (2007).
[22] J. Appel *et al.*, Proc. Natl. Acad. Sci. U.S.A. **106**, 10960 (2009).
[23] N. Sangouard *et al.*, Phys. Rev. A **77**, 062301 (2008).
[24] J. B. Brask *et al.*, Phys. Rev. A **81**, 020303(R) (2010).